

Deviation from Bloch's $T^{3/2}$ Law and Spin-Glass-Like Behavior in $\text{La}_{0.7}\text{Ca}_{0.3}\text{MnO}_3$ Nanoparticles

Tran Dang Thanh · D. H. Manh · N. X. Phuc ·
P. T. Phong · T. L. Phan · S. C. Yu

Received: 9 June 2014 / Accepted: 14 October 2014 / Published online: 26 October 2014
© Springer Science+Business Media New York 2014

Abstract Three samples of $\text{La}_{0.7}\text{Ca}_{0.3}\text{MnO}_3$ nanoparticles were prepared by a reactive milling method with the milling times $t_m = 8, 12,$ and 16 h. The studies based on X-ray diffraction and electron microscopes reveal that the mean particle size of nanoparticles is about 7 nm. Saturation magnetization values determined from fitting the Langevin function to the magnetization curve at 5 K decrease from 36.8 to 14.7 emu/g with increasing t_m from 8 to 16 h. Particularly, temperature dependences of saturation magnetization for these samples do not follow Bloch's $T^{3/2}$ law, but follow a T^ε law. The results obtained from investigating the DC magnetization and AC susceptibility indicate an existence of the spin-glass-like behavior in the samples, which is ascribed to the competition of ferromagnetic and anti-ferromagnetic interactions.

Keywords Perovskite-typed manganites · Nanoparticles · Magnetic and spin-glass-like properties

T. Dang Thanh (✉) · D. H. Manh (✉) · N. X. Phuc
Institute of Materials Science,
Vietnam Academy of Science and Technology,
18-Hoang Quoc Viet, Hanoi, Vietnam
e-mail: thanhxraylab@yahoo.com
e-mail: manhdh@ims.vast.ac.vn

P. T. Phong
Department of Natural Science, Nha Trang Pedagogic College,
Khanh Hoa, Vietnam

T. L. Phan · S. C. Yu (✉)
Department of Physics, Chungbuk National University,
Cheongju, 361-763, South Korea
e-mail: scyu@chungbuk.ac.kr

1 Introduction

It is known that lanthanum manganite (LaMnO_3) is an anti-ferromagnetic (anti-FM) insulator. Substituting a part of La by a metallic element (usually an alkaline-earth or alkali element) makes the doped materials exhibiting ferromagnetic (FM) metallic behaviors below the Curie temperature (T_C). The physical properties of manganites are arisen from two classes of competing effects: (i) super-exchange interactions cause insulating and anti-FM-ordered ground states, and (ii) double-exchange interactions lead to metallic and FM ordered ground states. These interactions can be tuned by external and internal parameters, such as temperature, magnetic field, the crystalline size, concentration of carriers, crystal-structure type, the size of ions, and so forth.

It is known that for perovskite manganites, when their size is reduced to the nanometer scale, they exhibit a number of outstanding physical properties; for example, low-field magnetoresistance, surface spin-glass (SG) behavior, super-paramagnetism (SPM), and low-field saturation magnetization [1–4]. These phenomena have promoted many research works on nanosized manganite materials. An exchange bias effect of magnetization and resistance relaxation at low temperatures for $\text{La}_{0.7}\text{Ca}_{0.3}\text{MnO}_3$ (LCMO) nano-ring network was found by Zhu et al. [2]. They suggested the existence of two SG types in the shell of LCMO grains, according to the core-shell model. Karmakar et al. [3] also observed the SG-like behavior in LCMO nanostructures at low temperatures. It was believed that the origin and nature of SG state in the nanostructured LCMO system were similar to the picture of hierarchical organization of metastable states. Evidences related to surface-spin freezing of nanopolycrystalline LCMO samples were observed by Dey and coworkers [4].

The glassy behavior at $T_S \approx 40$ K is attributed to competing magnetic interactions stabilized in a SG-like frozen state at the surface region of nanometric grains. However, physical mechanisms related to the SG phenomenon in LCMO nanoparticles are still a controversial issue. In this paper, we present a study on the deviation from the Bloch's $T^{3/2}$ law and the SG-like behavior in LCMO nanoparticles.

2 Experiment

Three LCMO nanoparticle samples denoted as S8, S12, and S16 were prepared by a reactive milling method with the milling times $t_m = 8, 12,$ and 16 h, respectively. Detailed descriptions of this method can be found elsewhere [5]. The crystal structure and particle size of samples were examined by X-ray diffraction (XRD) performed on a SIEMENS-D5000 diffractometer. The size and shape of nanoparticles were determined by using scanning electron microscopy (SEM, Hitachi S-4800) and high-resolution transmission electron microscopy (HR-TEM, Philips CM20-FEG). Measurements of the dynamic magnetic relaxation, AC susceptibility, and magnetization were carried out on a physical properties measurement system (PPMS 6000) with $T = 5$ – 300 K, $H = 0$ – 50 kOe, and $f = 297$ – 1337 Hz.

3 Results and Discussion

Room-temperature XRD patterns, Fig. 1a, revealed the single phase in an orthorhombic structure (the space group $Pnma$) of the samples [6]. Averaged crystallite sizes calculated by using the XRD data and Warren-Averbach method are about 8, 7, and 6 nm for S8, S12, and S16, respectively. Figure 1b shows a representative SEM image for S8 (particle-size distributions are similar to the other samples), where the average particle size is about 15 nm. This size is quite larger than that obtained from the XRD and HR-TEM studies (notably, for the HR-TEM study, the averaged particle size of nanoparticles is about 7 nm, Fig. 1c). This could be explained by a high level of lattice disorders (marked as \uparrow), including dislocations (marked as \perp) at the faceted grain surface of nanocrystals, as can be seen in Fig. 1c.

Following the structural analyses, we have investigated the magnetic properties of these nanoparticle samples. Figure 2a shows their temperature dependences of field-cooled (FC) and zero-field-cooled (ZFC) magnetizations, $M_{ZFC/FC}(T)$, for the field $H = 10$ Oe. These $M_{ZFC}(T)$ curves are similar to those recorded for SG and/or SPM systems. They exhibit a peak at the blocking temperature (T_B), which is shifted towards lower temperatures with increasing t_m ($T_B = 87, 76,$ and 63 K for $t_m = 8, 12,$ and 16 h, respectively). With decreasing temperature, meanwhile, $M_{FC}(T)$

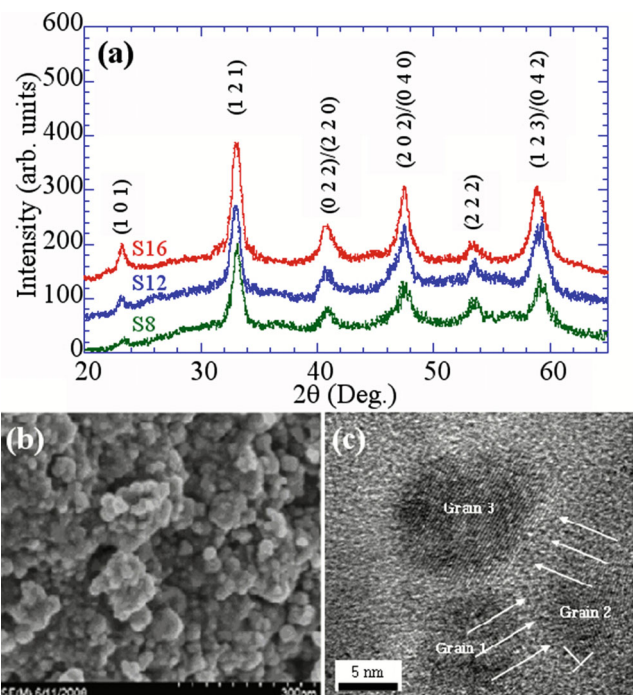


Fig. 1 a XRD patterns of the samples S8, S12, and S16, where the XRD peaks are marked with the Miller indices, after ref. [6]. b SEM image and c HR-TEM image for a representative sample 8. Arrows indicate lattice disorders and *inverted letter T* indicates dislocations

firstly increases, and then saturates to a constant value. Such the features indicate that our LCMO nanoparticles have the SG-like behavior [7]. Furthermore, magnetization variations in the paramagnetic (PM) region for the samples can be analyzed by using the CurieWeiss law [8], $\chi(T) = C/(T - \theta)$, where C and θ are the Curie constant and Curie-Weiss temperature respectively. It appears in Fig. 2b that the $\chi^{-1}(T)$ curves exhibit the linear behavior with two distinct slopes. The first one (denoted as R1) is related to the FM transition temperature while the other (denoted as R2) is located at a higher temperature. The C and θ values obtained from fitting the $\chi(T)$ data to the Curie-Weiss law are $C_1 = 0.76, 1.31,$ and 1.34 emu·K/mol and $\theta_1 = 178, 168,$ and 137 K

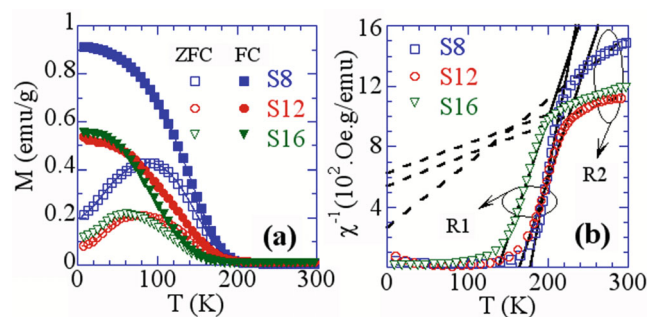


Fig. 2 a $M(T)$ curves for $H = 10$ Oe and b $\chi^{-1}(T)$ curves for S8, S12, and S16. In b, the solid and dashed lines are the fitting curves of the $\chi^{-1}(T)$ data to the CurieWeiss law in the regions R1 and R2

in the region R1; $C_2 = 5.02, 9.92,$ and 10.90 emu-K/mol and $\theta_2 = -63, -241,$ and -323 K in the region R2 for S8, S12, and S16, respectively. Here, the C_1 values are comparable to the theoretical one with $C = 0.97$ emu-K/mol corresponding to PM Mn ions with an average valence of 3.35 (i.e., the mixture of Mn^{3+} and Mn^{4+} ions) [9]. The decrease of θ_1 with increasing t_m reflects the weakening of FM interactions in LCMO nanoparticles. The appearance of the region R2 with negative θ_2 values suggests a strong anti-FM nature which is mainly related to superexchange interaction pairs $Mn^{4+}Mn^{4+}$ and $Mn^{3+}Mn^{3+}$. Therefore, magnetic moments become difficult to reach a saturation state, as can be seen in Fig. 3a.

Quantitatively field dependences of magnetization, $M(H)$ are further analyzed by using the SPM theory initiated by Langevin. According to Ningthoujam et al. [10], if there is a PM fraction in addition to SPM particles, temperature and field dependences of magnetization can be written as

$$M = M_S \left[\coth \left(\frac{\mu H}{k_B T} \right) - \left(\frac{k_B T}{\mu H} \right) \right] + \chi H, \quad (1)$$

where M_S and μ are the saturation magnetization and magnetic moment of an individual SPM particle, respectively. As shown in Fig. 3a, the $M(H)$ data recorded at 5 K were fitted well with (2), see the solid lines. Obtained M_S values are 36.77, 19.42 and 15.16 emu/g for S8, S12, and S16, respectively. These values are much smaller than that of a bulk LCMO sample with $M_S = 97.5$ emu/g [11]. The decrease of M_S in LCMO nanoparticles is ascribed to the existence of a nonmagnetic or AFM layers on the surface that their thickness increases with increasing t_m .

Figure 3b shows the behavior of the M_S versus temperature for the samples, where M_S values obtained upon fitting the magnetization data at 5 K to (2). In general, the thermal dependence of magnetization for nanoparticles deviates from expected Bloch's $T^{3/2}$ law when magnons with a wavelength longer than the particle diameter can not be excited, and a threshold of thermal energy is required

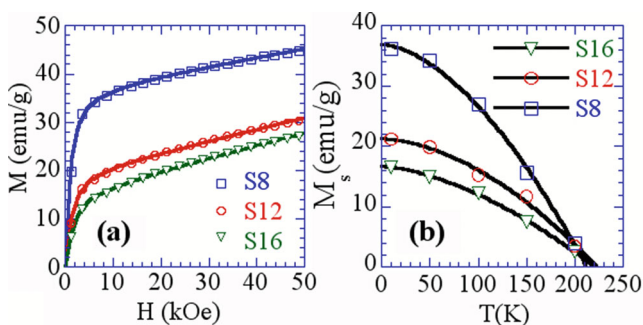


Fig. 3 **a** $M(H)$ data at 5 K are fitted to (2) and **b** $M_S(T)$ data are the fitted to a function $M_S = M_0(1 - BT^\epsilon)$. The solid lines are the fitting curves

to generate spin waves [12]. In our case, the temperature dependence of M_S does not follow Bloch's $T^{3/2}$ law, but obeys a T^ϵ law with ϵ increasing from 1.69 to 1.76 if t_m increases from 8 to 16 h, see the solid lines shown in Fig. 3b. A slightly greater value of ϵ compared to the bulk sample value ($\epsilon = 3/2$) [13] is due to the effect related to small particle sizes.

To further understand the SG-like behavior existing in the samples, we have measured the AC susceptibility (χ_{AC}) as the function of temperature under an AC applied field of 10 Oe at different frequencies ($f = 297$ –1337 Hz). Figure 4a shows the AC susceptibility (consisting of real χ' and imaginary χ'' parts) for a representative frequency $f = 897$ Hz. One can see that the peak temperature (denoted as the freezing temperature T_f) decreases with increasing t_m . For each sample, T_f shifts towards higher temperatures when frequency increases, see Fig. 4b–d. This is a typical feature of a conventional SG system [14]. Additionally, to distinguish between SG and SPM systems, the c parameter is considered as an empirical criterion [15]. This parameter can be defined by

$$c = \frac{\Delta T_f}{T_f \Delta (\log_{10} f)}, \quad (2)$$

where ΔT_f and $\Delta(\log_{10} f)$ are the shifts of T_f and $\log_{10} f$, respectively. Normally, c is about 10^{-2} for a conventional SG system, whereas $c \geq 0.1$ for SPM [16]. In our case, the obtained c values are 0.062, 0.055, and 0.051 for the

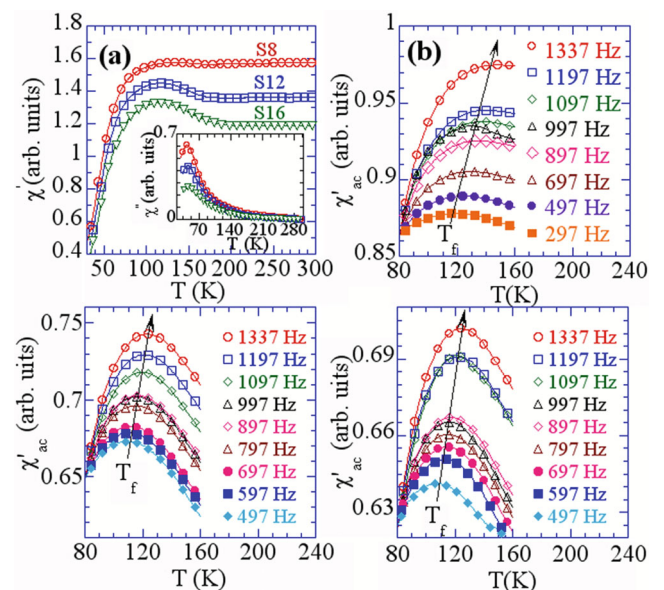


Fig. 4 Temperature dependences of the real part of the AC susceptibility in an AC magnetic field $H_{AC} = 10$ Oe for the samples measured at 897 Hz (**a**), and at different frequencies for the samples S8 (**b**), S12 (**c**), and S16 (**d**). The inset in **a** shows the image part of the AC susceptibility at 897 Hz for the samples. Arrow denotes the variation trend of T_f

samples S8, S12, and S16, respectively. Such the results prove that our LCMO nanoparticles at low temperatures exhibit the SG-like behavior rather than the SPM behavior. The existence of the SG-like state is considered as a consequence of competing magnetic interactions (between anti-FM and FM phases) and of spin frustration at surface layers of LCMO nanoparticles. A similar feature was observed in bilayer heterostructures composed of anti-FM SrMnO₃ and FM L_{0.7}Sr_{0.3}MnO₃ [1].

4 Conclusion

LCMO nanoparticles with the averaged crystallite size of ~7 nm prepared by a reaction milling method were carefully studied by measurements of the DC magnetization and AC susceptibility. Both the magnetization and T_B values decrease with increasing t_m . We believe that the magnetization decrease is attributed to the thickness of nonmagnetic or anti-FM layers on the surface of LCMO nanoparticles, which increases with increasing t_m . Temperature dependences of saturation magnetization obeys a T^ε law (with $\varepsilon = 1.69$ – 1.76). Interestingly, our studies indicate the existence of the SG-like behavior in the samples, which is originated from magnetic frustration at the surface of nanoparticles.

Acknowledgments This work was supported by the National Foundation for Science and Technology Development (NAFOSTED) under Grant Number of 103.02-2012.57 in Vietnam and by the Converging Research Center program through the Ministry of Science, ICT and Future Planning, Korea (2014048835). A part of the work was done in the Key Laboratory for Electronic Materials and Devices, Institute of Materials Science, VAST, Vietnam.

References

- Ding, J.F.O., Lebedev, I., Turner, S., Tian, Y.F., Hu, W.J., Seo, J.W., Panagopoulos, C., Prellier, W., Van Tendeloo, G., Wu, T.: Interfacial spin glass state and exchange bias in manganite bilayers with competing magnetic orders. *Phys. Rev. B* **87**, 054428 (2013)
- Zhu, M.H., Zhao, Y.G., Cai, W., Wu, X.S., Gao, S.N., Wang, K., Luo, L.B., Huang, H.S., Lu, L.: Spin-glass shell and magnetotransport properties of a La_{0.67}Ca_{0.33}MnO₃ nanoring network. *Phys. Rev. B* **75**, 134424 (2007)
- Karmakar, S., Chaudhuri, B.K., Chan, C.L., Yang, H.D.: Origin of low temperature memory and aging effects in spin glass like La_{0.7}Ca_{0.3}MnO₃ nanomanganite. *J. Appl. Phys.* **108**, 113916 (2010)
- Dey, P., Nath, T.K., Manna, K., Yusuf, S.M.: Enhanced grain surface effect on magnetic properties of nanometric La_{0.7}Ca_{0.3}MnO₃ manganite: evidence of surface spin freezing of manganite nanoparticles. *J. Appl. Phys.* **104**, 103907 (2008)
- Manh, D.H., Thanh, T.D., Phuc, N.X., Hong, L.V., Phong, P.T., Hung, L.T.: Perovskite nanoparticles synthesised by reactive milling combined with thermal processing: preparation, morphology and structure characterisation. *Int. J. Nanotechnol.* **8**, 241 (2011)
- International Centre for Diffraction Data, PDF card number 49–0416 (1997)
- Suzuki, M., Fullem, S.I., Suzuki, I.S.: Observation of superspin-glass behavior in Fe₃O₄ nanoparticles. *Phys. Rev. B* **79**, 024418 (2009)
- Kittel, C. *Introduction to Solid State Physics*, 7th ed. Wiley, New York (2000)
- Borges, R.P., Ott, F., Thomas, R.M., Skumryev, V., Coey, J.M.D., Arnaud, J.I., Ranno, L.: Field-induced transition in the paramagnetic state of (Sm_{0.65}Sr_{0.35})MnO₃ associated with magnetic clusters. *Phys. Rev. B* **60**, 12847 (1999)
- Ningthoujam, R.S., Gajbhiye, N.S.: Magnetization studies on ε -Fe_{2.4}Co_{0.6}N nanoparticles. *Mater. Res. Bull.* **45**, 499 (2010)
- Song, H., Kim, W., Kwon, S.J., Kang, J.: Magnetic and electronic properties of transition-metal-substituted perovskite manganites-La_{0.7}Ca_{0.3}Mn_{0.95}X_{0.05}O₃ (X=Fe, Co, Ni). *J. Appl. Phys.* **89**, 3398 (2001)
- Mandal, K., Mitra, S., Anil Kumar, P.: Deviation from Bloch $T^{3/2}$ law in ferrite nanoparticles. *Europhys. Lett.* **75**, 618 (2006)
- Hendriksen, P.V., Linderth, S., Lindgard, P.A.: Finite-size modifications of the magnetic properties of clusters. *Phys. Rev. B* **48**, 7259 (1993)
- Chen, D.X., Skumryev, V., Coey, J.M.D.: Domain-wall dynamics in aligned bound Sm₂Fe₁₇. *Phys. Rev. B* **53**, 15014 (1996)
- Liu, D.L., Du, F., Wei, Y.J., Wang, C.Z., Huang, Z.F., Meng, X., Chen, G., Chen, Y., Feng, S.H.: Spin-glass state in hexagonal Li_{2.5}Co_{0.5}N. *Mater. Lett.* **63**, 133 (2009)
- Wang, Y.T., Bai, H.Y., Pan, M.X., Zhao, D.Q., Wang, W.H.: Multiple spin-glass-like behaviors in a Pr-based bulk metallic glass. *Phys. Rev. B* **74**, 064422 (2006)